Journal of Mining and Earth Sciences
Website: https://jmes.humg.edu.vn

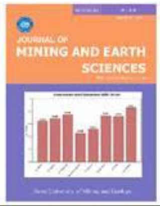

Comparative assessment of iRIC-Morpho2DH and RAMMS-DF for debris-flow using integrated field investigation and model validation: A case study at Tra Leng commune, Vietnam

Lan Chau Nguyen[1,*], Kien Van Vu[2], Nghia Tuan Do[2]

[1] *University of Transport and Communications, Hanoi, Vietnam*
[2] *Thuy Loi University, Hanoi, Vietnam*

ARTICLE INFO

Article history:
Received 15th Apr. 2026
Revised 25th Jun. 2026
Accepted 5th Jul. 2026

Keywords:
CU test,
Debris flow,
Hazard Assessment,
iRIC-Morpho2DH,
Model Comparison,
RAMMS-DF,
Tra Leng,
UAV.

ABSTRACT

On 28 October 2020, an intense rainfall event triggered a destructive debris-flow disaster in Hamlet 1, Tra Leng Commune, Vietnam, resulting in severe damage, including the destruction of 14 houses and 22 fatalities or missing persons. This study proposes an integrated investigation framework that combines UAV-derived photogrammetry to generate a 1 m-resolution Digital Elevation Model (DEM), subsurface characterization from two 20 m-deep boreholes supported by comprehensive laboratory testing, and comparative runout modeling using the iRIC-Morpho2DH and RAMMS-DF debrisflow simulation models. Field investigations identified three major landslide source zones located upstream of the deposition area. The iRIC-Morpho2DH model successfully reproduced the temporary natural-dam formation and breach process, yielding a peak flow velocity of 13.28 m/s and a maximum flow depth of 8.70 m within the deposition zone. The RAMMS-DF model produced a peak velocity of 15.12 m/s, a maximum flow depth of 8.1 m within the deposition zone, 22.72 m (upper gorge), and a peak dynamic pressure of 438.9 kPa under the optimal parameters μ = 0.205 and ξ = 50 m/s^2. Both models accurately predicted the complete inundation extent of all 14 destroyed houses and showed good agreement with post-event field observations. The results indicate that iRIC-Morpho2DH is better suited for analyzing short-term dynamic processes, such as flow blockage and dam breach. In contrast, RAMMS-DF is more effective for deposition mapping and infrastructure impact assessment for hazard zoning.

*Corresponding author
E - mail: nguyenchaulan@utc.edu.vn
DOI: 10.46326/JMES.2026.67(4).09

1. Introduction

Debris flows are gravity-driven mixtures of water, sediment, and rock debris, characterized by viscous-plastic rheology, flow velocities up to 15 m/s, and peak discharges that can exceed those of equivalent-recurrence clear-water floods by 40÷50 times due to progressive sediment entrainment (Iverson et al., 2003; Iverson, 1997; Jakob et al., 2005; 2012; Takahashi, 1978). In the mountainous regions of Southeast Asia, extreme monsoon rains have continuously caused chain hazards, from initial landslides to the formation of debris runoff and downstream deposition, with serious consequences to the area (Bui et al., 2026; Chen & Wang, 2017; Chen et al., 2024; He et al., 2021; Imaizumi et al., 2017; Lan et al., 2024).

The mountainous western region of Da Nang City is a typical example of high vulnerability to debris-flow hazards. The areas of Phuoc Son, Bac Tra My, and Nam Tra My (formerly part of Quang Nam Province and now administratively incorporated into Da Nang City) have seen a significant increase in debris-flow frequency in recent years. In Bac Tra My alone, the annual number of debris-flow events rose from approximately 5÷7 per year during 2000÷2010 to 15÷18 per year during 2021÷2023. This trend is primarily associated with intensified typhoon-induced rainfall, progressive deforestation, and the expansion of road infrastructure that destabilizes deeply weathered hillslopes. On 28 October 2020, Typhoon Molave produced 199.6 mm of rainfall in a single day over catchments that had already accumulated approximately 1,530 mm of rainfall throughout October 2020, triggering a multi-source landslide cascade in Tra Leng Commune, Da Nang City. The event buried 14 houses and resulted in 22 fatalities and missing persons (Bui et al., 2026; Lan et al., 2024).

A reliable numerical simulation of debris flows requires accurate prediction of runout paths, flow depth, velocity, and final deposition extent from identified source areas and mobilized volumes. Currently, two major modeling approaches are widely used. The first group comprises depth-averaged non-Newtonian continuum models, represented by iRIC-Morpho2DH (Takebayashi & Fujita, 2020), which can simulate mass exchange between the flowing debris and the erodible channel bed while effectively reproducing transient dynamic processes, such as temporary natural-dam formation and breach. The second group includes semi-empirical Voellmy–Salm friction-based models, represented by RAMMS-DF (Abraham et al., 2022; Ahmad et al., 2025; Bui et al., 2026; Mikoš & Bezak, 2021), which are widely used for debris-flow runout assessment and hazard zonation.

Despite the growing body of literature on individual applications of these models, rigorous comparative assessments quantifying the relative strengths, limitations, and complementarity of iRIC-Morpho2DH and RAMMS-DF for the same well-documented tropical debris-flow event remain scarce. A comparative evaluation of iRIC-Morpho2DH and RAMMS-DF is important because model selection for practical debris-flow hazard assessment is often constrained by data availability, computational cost, and the intended application of the results. The 2020 Tra Leng event is a well-documented case for such an assessment, supported by multi-temporal UAV surveys, two 20 m-deep boreholes, laboratory test data, including Soil–Water Characteristic Curve measurements, post-event damage documentation, and eyewitness accounts of the disaster's timing. On this basis, the present study has three specific objectives: (1) to reconstruct the post-event terrain at 1 m resolution using UAV photogrammetry; (2) to characterize the subsurface stratigraphy and geotechnical properties through borehole investigation and laboratory testing; and (3) to compare the runout behavior simulated by iRIC-Morpho2DH and RAMMS-DF, with emphasis on their relevance to early-warning development and structural hazard mitigation.

2. Study area

2.1. Location, topography, and climate

The study area (approximately 15°29′N, 107°59′E) is located in Hamlet 1, Tra Leng Commune, Da Nang City. The catchment drains westward into the Thu Bon River system. Elevation ranges from about 160 m above sea level at the Leng River confluence to 1,966 m at the watershed divide, with an average channel gradient of about 35% along the 1.9 km debris-flow corridor (Figure 1).

Slope gradients exceed 30^0 across most of the catchment and locally reach 45÷60^0 on bedrock-controlled scarps above 800 m above sea level (a.s.l.). Mean annual rainfall exceeds 3,000 mm and is primarily concentrated during the typhoon season from October to December.

2.2. Rainfall trigger

October 2020 was exceptionally wet across central Vietnam. At the Tra My reference gauge, October rainfall totaled approximately 1,530 mm. An initial episode on 11 October 2020 delivered nearly 450 mm in 24 hours, saturating the weathered mantle and raising antecedent pore-water pressures. On 28 October, rainfall intensities ranged from 15.6 to 41.4 mm/h, yielding a daily total of 199.6 mm (Figure 2). This heavy rain is the direct cause of the landslide,

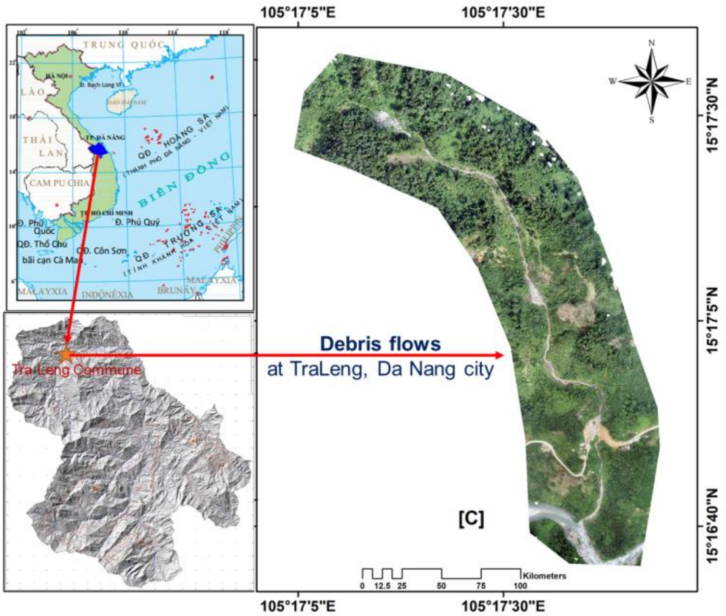

Figure 1. Study location of the Tra Leng debris-flow event, Da Nang City.

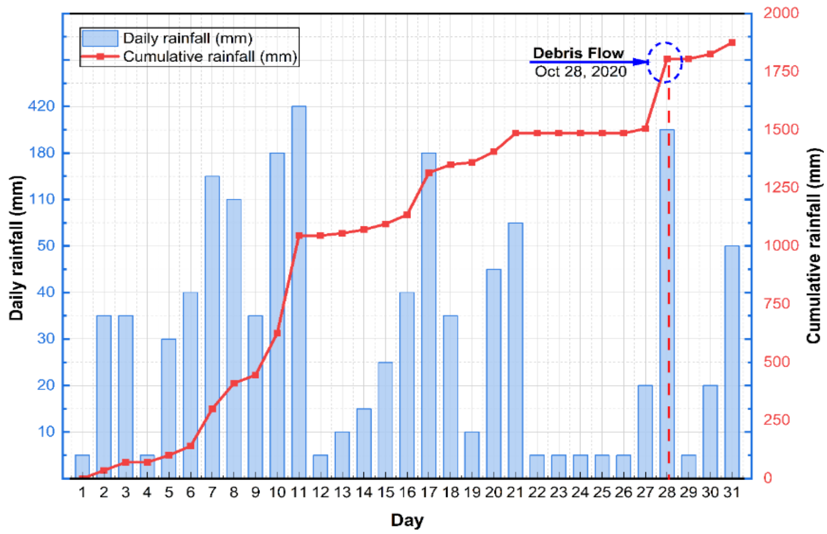

Figure 2. Accumulated rainfall chart at Tra My station in October 2020 (Lan et al., 2024).

thereby leading to the flow of mud and stones. The fact that long periods of rain, followed by heavy rain in a short period, often trigger debris flows in tropical areas.

2.3. Geology and geomorphology

The bedrock comprises Precambrian metamorphic schists and phyllites (Kham Duc Formation), foliated granitoids (Chu Lai Complex), and migmatitic gneisses (Dak My and Tra Bong complexes), intersected by NW-SE and NE-SW fault zones. A high proportion of hillslopes lie within 500 m of mapped fault traces, where fracturing and hydrothermal alteration substantially degrade rock-mass quality. Thick lateritic and saprolitic weathering profiles (2÷14 m) overlie the fractured bedrock, creating conditions of elevated hydraulic conductivity contrast at the soil-rock interface. Three discrete landslide headscarps were identified from UAV imagery at 0.20 km, 0.62 km, and 1.35 km upstream of the deposition fan. Post-event surface lowering of 10÷15 m was documented in the upper transport reach; the deposition zone, covering approximately 14.51 ha over the residential area of Hamlet 1, showed fill depths of 8÷10 m.

3. Materials and methods

3.1. UAV photogrammetric survey

Post-event UAV surveys were conducted during the reconnaissance phase in January 2021 and again in July 2024 to obtain high-resolution terrain data for the affected catchment. The UAV platform was equipped with an RGB camera and captured overlapping aerial images with a ground sampling distance of approximately 5÷10 cm. Image acquisition was planned with at least 80% overlap to ensure reliable photogrammetric reconstruction (Figure 3).

The aerial images were processed using Agisoft Metashape. This program produced a bare-earth DEM at 1 m spatial resolution, covering the entire 1.9 km debris-flow corridor. For numerical modeling, the DEM was resampled to 10 m for the iRIC-Morpho2DH simulation, while the original 1 m DEM was retained for RAMMS-DF. This high-resolution topographic dataset serves as the basis for identifying the source zone, mapping the flow path, and validating the simulated sedimentation extent against geomorphological evidence recorded during field mapping.

Figure 3. TraLeng debris fan and damaged infrastructure (UAV picture).

3.2. Geotechnical investigation and laboratory testing

In August 2024, two geotechnical boreholes, BH1 and BH2, were drilled to a depth of 20 m to investigate subsurface conditions at the study site. Standard Penetration Tests were conducted at 1.5 m depth intervals, and the drilling program yielded 17 soil samples and 4 rock specimens for subsequent laboratory characterization. The stratigraphic profile comprises: Layer edQ (colluvial deposit), encountered only in BH2 with a thickness of 2.1 m, consisting of stiff, plastic, gravelly clay; Layer IA1 (highly weathered zone), composed of semi-hard weathering products with thicknesses ranging from 2.0 to 13.9 m; Layer IA2 (strongly weathered zone), consisting of weak to moderately strong gneiss with intense open fracturing and iron-oxide coatings; Layer IB (moderately weathered zone), comprising strong, highly fractured gneiss with open discontinuities, where drill cores were mainly recovered as fragments and blocks; Layer IIA (fractured rock zone), encountered only in BH1 with a thickness of 5.0 m, consisting of strong to very strong, slightly weathered gneiss with moderately to highly fractured, closed discontinuities and calcite coatings; and Layer IIB (relatively intact rock zone), composed of very strong, relatively intact gneiss with few closed fractures and calcite-coated, rough surfaces. Laboratory testing included grain-size analysis, Atterberg limits, index properties, UU and CU triaxial compression tests, oedometer consolidation tests, and uniaxial compressive strength (UCS) tests under both dry and saturated conditions, in accordance with Vietnamese Standards (TCVN) and ASTM standards. A summary of the geotechnical properties is presented in Table 1.

3.3. Debris-flow runout simulation: iRIC-Morpho2DH

The module is a depth-averaged two-dimensional model that treats debris flow as a continuous, incompressible, viscoplastic (non-Newtonian) fluid under shallow-water assumptions (Takebayashi & Fujita, 2020). The depth-averaged continuity equation is:

$$\frac{\partial h}{\partial t} + \frac{\partial (hu)}{\partial x} + \frac{\partial (hv)}{\partial y} = \frac{E}{c^*} \quad (1)$$

Where h is debris-flow depth (m); u and v are depth-averaged velocities in the x and y directions (m/s); c^* is the sediment concentration in the deposit; and E is the bed erosion velocity (m/s). The momentum equations include terms for bed slope, hydrostatic pressure, and basal shear stress. The yield stress τy is computed as follows (Takahashi, 1978), and the volumetric sediment concentration Cv is computed from the slope angle, sediment density, water density, and internal friction angle. A major advantage of the iRIC-Morpho2DH formulation is that it explicitly represents the interaction between the moving debris mass and the erodible channel bed. This treatment enables the model to account for sediment entrainment, temporary flow blockage, natural dam development, and subsequent breaching during debris-flow propagation. The model was simulated using a 1 m DEM, a 10 m × 10 m computational grid, three source areas, 14 building obstacles, vegetation resistance (5 m spacing, 2.0 m height), and a 500-second simulation duration.

Table 1. Geotechnical parameters for the principal soil layers.

Parameter	Layer edQ	Layer IA1
Water content, w (%)	26.03	22.75
Unit weight, γ (kN/m^3)	19.0	19.2
Specific gravity, Gs	2.71	2.70
Void ratio, e	0.795	0.725
Liquid limit, LL (%)	33.34	32.00
Plasticity index, PI (%)	11.48	10.98
Cohesion (direct shear), c (kPa)	21.6	23.3
Friction angle (direct shear), φ (^{0})	$16^0 22'$	$18^0 43'$
Effective cohesion, c' (CU triaxial, kPa)	16.10	18.95
Effective friction angle, φ' (CU triaxial, ^{0})	$29^0 10'$	$30^0 33'$

3.4. Debris-flow runout simulation: RAMMS-DF

RAMMS-DF (Rapid Mass Movement Simulation, SLF Switzerland) models the debris mass as a depth-averaged continuum governed by the Voellmy-Salm friction law (Ahmad et al., 2025; Bui et al., 2026; Singh et al., 2025). The total frictional resistance S (Pa) can be decomposed into velocity-independent (Coulomb) and velocity-dependent (turbulent) components:

$$S = \mu \rho h g \cos(\phi) + \frac{\rho g u^2}{\xi} \quad (2)$$

Where μ (dimensionless) is the Coulomb friction coefficient; ρ (kg/m^3) is the bulk density; h (m) is the local flow depth; g (m/s^2) is the gravitational acceleration; ϕ (^{0}) is the local terrain slope; u (m/s) is the depth-averaged velocity; and ξ (m/s^2) is the viscous-turbulent friction coefficient. In this paper, the model was run using the 1 m DEM.

The Coulomb coefficient μ = 0.205 was estimated by back-analysis as tan(α), where α = 12^0 is the mean depositional fan gradient. ξ characterizes the flow's turbulent behavior. Typically, small values of ξ are reported for granular flows, whereas relatively large ξ values are sometimes associated with muddy flows. The initial values of the Voellmy friction coefficients recommended in the RAMMS-DF model suggest that the viscous–turbulent friction coefficient ξ [m/s^2] ranges from 50÷200 m/s^2 for debris flows and from 200÷1.000 m/s^2 for mud flows. Under the conditions at Tra Leng, field investigations indicated that the three main landslide source zones transported large volumes of loose, coarse-grained material, including several boulders up to 10 m in diameter. The optimal parameters (μ = 0.205, ξ = 50 m/s^2) were used in the simulation in this paper.

4. Results

4.1. iRIC-Morpho2DH simulation results

The iRIC-Morpho2DH model reproduces a four-stage cascading hazard mechanism consistent with field evidence. The initial landslide at Source Zone 1 initiated the debris flow at t = 0 s. At approximately t = 102 s, the advancing surge destabilized Source Zone 2, triggering a secondary failure and increasing the total flow discharge. At t = 122 s, the combined flow further destabilized Source Zone 3, located approximately 200 m upstream of the deposition area.

At t = 157 s, the debris flow passed through a channel constriction and reached the fan-shaped depositional area approximately 0.23 km downstream. However, the flow became discontinuous and temporarily stopped. Field investigations indicated that the constricted channel section formed a temporary natural dam, with an upstream impounded depth of 5.63 m. (Figure 4).

After nearly 100 s, the debris flow breached the temporary dam at t = 253 s, releasing a surge with a peak velocity of 13.28 m/s and a maximum flow depth of 8.70 m across the depositional fan (Figure 5). The iRIC-Morpho2DH model predicted a maximum flow depth of 21.76 m. All 14 residential houses were within the simulated inundation area. The main active phase of the debris flow ended at t = 500 s. The formation and subsequent failure of the natural dam were critical features of the simulated hazard scenario; sensitivity simulations without the temporary dam showed peak velocities approximately 35% lower.

4.2. RAMMS-DF simulation results

The RAMMS model depends on the friction parameter pair μ−ξ for debris-flow simulation. As presented in Section 3.4, the Coulomb friction coefficient was set to μ = tan(12^0) = 0.205, while the viscous–turbulent friction coefficient ξ = 50 m/s^2 represents turbulent flow resistance during debris-flow propagation. The results indicate that the turbulent friction term is the primary control on the spatial extent of deposition in this narrow, steep-walled channel. With the optimal parameters, RAMMS-DF yields Vmax = 15.12 m/s, Hmax = 22.72 m, and Pmax = 438.9 kPa (Figure 6). Peak values are concentrated in the steep upper transit reach. (channel gradient > 40^0, approximately 800÷1,200 m upstream), with progressive attenuation toward the fan. Maximum flow heights over the residential zone reach 8.1 m (Figure 6a); simulated dynamic pressures of 200÷440 kPa confirm the potential for catastrophic structural damage to reinforced-

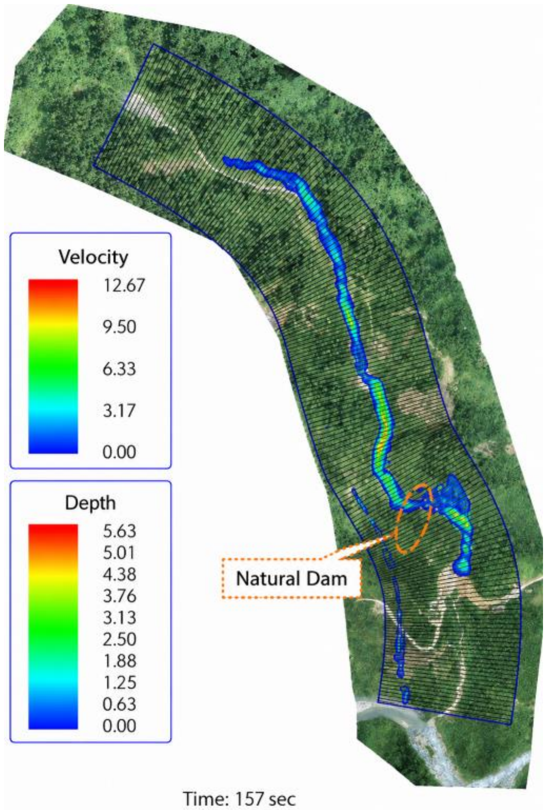

Figure 4. Depth of debris flow and position of natural dam after 157 s of simulation.

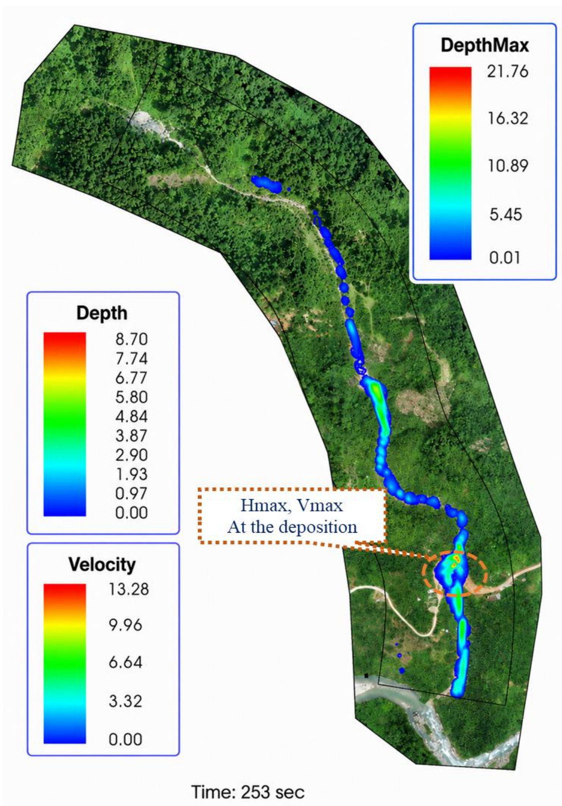

Figure 5. Velocity and depth of debris flow simulation after 253 s of simulation.

concrete buildings. The infrastructure impact assessment identifies 14 houses completely inundated (flow height > 2 m), 6 partially impacted (0.5÷2 m), 122.51 m of primary road destroyed, and approximately 14.51 ha of total land area impacted (Figure 6).

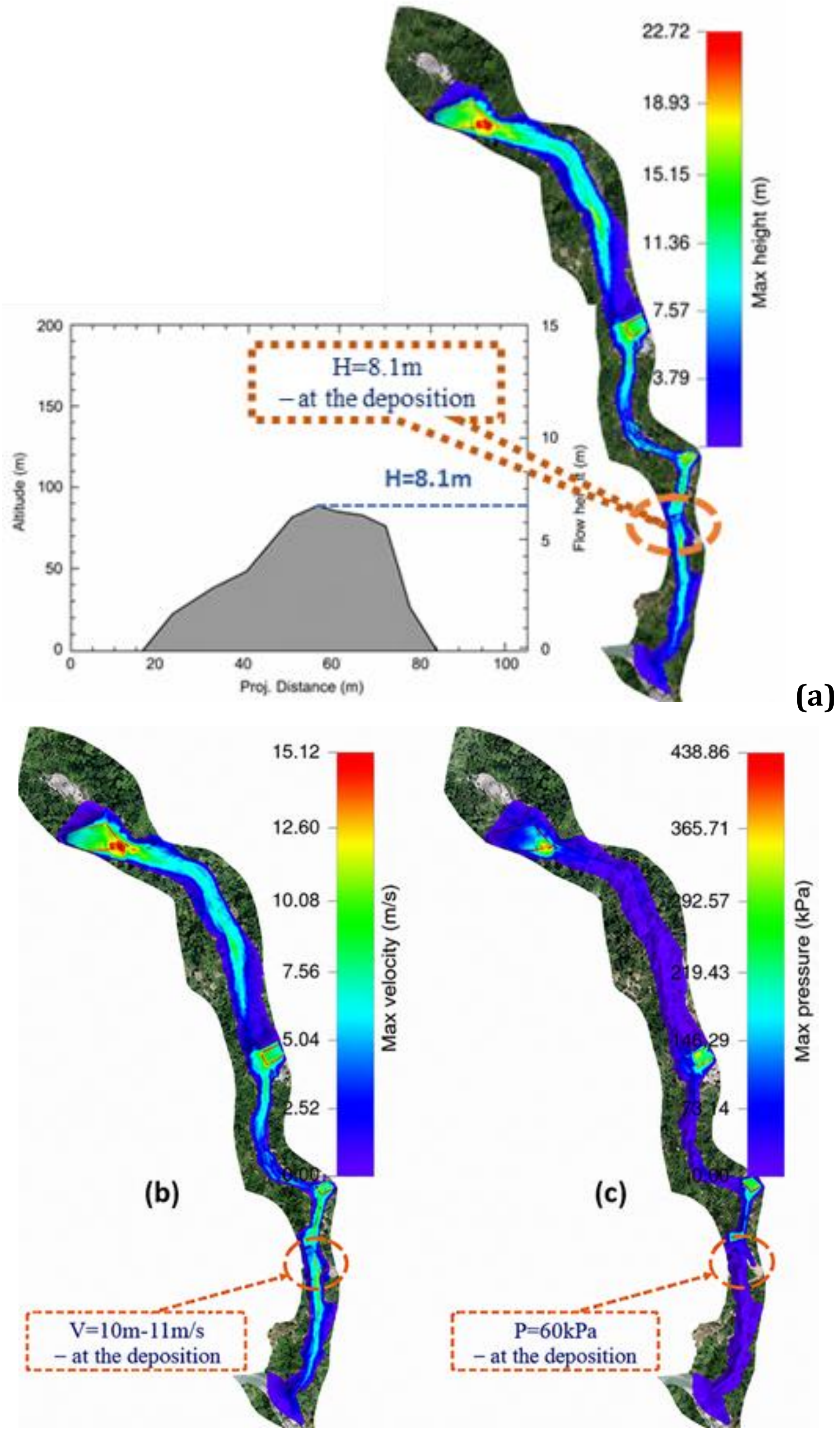

Figure 6. Depth (a), Velocity (b), and Pressure (c) of debris flow, with the positions of damaged houses (RAMMS simulation).

5. Comparative assessment of iRIC-Morpho2DH and RAMMS-DF

5.1. Model philosophy and governing equations

The two runout codes differ fundamentally in how they model debris-flow rheology and mass exchange with the bed. iRIC-Morpho2DH uses a non-Newtonian viscoplastic formulation and explicitly incorporates interactions between the moving debris mass and the erodible channel bed through the mass-balance term E/c*. This enables the model to simulate entrainment, temporal changes in sediment concentration, variations in bulk density, and bed-elevation adjustment during the event. This formulation is highly relevant to tropical debris-flow systems, where progressive entrainment and bulking over steep, channelized reaches can markedly increase flow volume and enhance downslope mobility. (Takahashi, 1978, 2009). By contrast, RAMMS-DF uses the Voellmy–Salm friction approach, in which flow resistance is represented by two empirical parameters: the Coulomb friction coefficient μ and the viscous–turbulent coefficient ξ. This framework treats the debris mass as a single aggregate and neither explicitly distinguishes rheological states nor accounts for bed erosion and sediment entrainment. These conceptual differences explain the contrasting outputs of the two models, particularly for peak flow depth, velocity distribution, and the simulation of temporary blockages and dam-breach processes (Ahmad et al., 2025; Bui et al., 2026; Takahashi, 1978, 2009; Takebayashi & Fujita, 2020).

5.2. Key output differences

The differences in simulated outputs between iRIC-Morpho2DH and RAMMS-DF primarily stem from how each model represents channel constriction and short-duration blockage–breach dynamics. The iRIC-Morpho2DH simulation resolved a temporary ponding condition about 0.23 km upstream of the fan, where flow depth increased to 5.63 m before the impounded material was released as a breach-generated surge with a maximum velocity of 13.28 m/s. By contrast, RAMMS-DF, which does not explicitly simulate dam-breach behavior, estimated a higher system-wide peak velocity of 15.12 m/s and a maximum flow depth of 22.72 m, both of which were mainly localized within the steep upper transport section.

Despite these differences, both models accurately reproduced the complete inundation of the 14 destroyed houses and produced flow depths in the fan area consistent with post-event field evidence. A key advantage of RAMMS-DF is its ability to provide spatially distributed dynamic pressure outputs. The estimated maximum pressure of 438.9 kPa provides useful information for evaluating building vulnerability and potential structural damage, information not directly available from the iRIC-Morpho2DH outputs.

5.3. Strengths and limitations

iRIC-Morpho2DH is well-suited to examining debris-flow processes in which sediment entrainment, changes in sediment concentration, and yield-stress variation strongly influence flow mobility. Owing to its physically based formulation, the model can represent time-dependent processes such as channel obstruction, temporary natural-dam formation, and subsequent dam breaching. For the Tra Leng event, iRIC-Morpho2DH provided a reasonable reconstruction of the multi-stage cascading process and indicated that the breach-induced surge played a key role in the event's most destructive phase. However, several limitations remain. First, the 10 × 10 m computational mesh is not sufficiently fine to accurately resolve narrow gorge cross-sections, where the maximum flow depth and velocity are concentrated. Second, the model does not explicitly generate dynamic-pressure results, limiting its utility for evaluating structural exposure, impact loading, and vulnerability. In addition, the physically based, process-oriented formulation increases computational demand relative to RAMMS-DF. Lastly, the model evaluation in this study relied primarily on qualitative correspondence with observed field evidence rather than on a formal quantitative validation criterion.

RAMMS-DF provides an efficient framework for debris-flow runout modeling and hazard mapping, particularly when detailed terrain representation is possible with high-resolution

DEMs. For the Tra Leng case study, the adopted μ–ξ friction parameters were selected through an integrated assessment of laboratory test results, field observations, local terrain morphology, and prevailing material characteristics. The model provides spatially distributed outputs of flow depth, velocity, and dynamic pressure, which are useful for infrastructure impact assessment, damage estimation, and land-use planning. Nevertheless, RAMMS-DF has important limitations. First, the Voellmy–Salm friction framework assumes a relatively uniform rheological behavior throughout the moving mass. Second, bed erosion and mass exchange between the flow and the channel bed are not explicitly simulated; therefore, progressive channel bulking cannot be fully captured. Third, transient processes such as temporary dam formation and dam breaching are not directly resolved. Fourth, reliable calibration generally requires mapped deposition extent or post-event field evidence from previous or well-documented debris-flow events.

5.4. Complementarity and recommended workflow

The two codes are best viewed as complementary rather than competing tools. A recommended integrated workflow for debris-flow hazard assessment in comparable tropical highland settings is: (1)iRIC-Morpho2DH: Use source volumes derived from field surveys, in combination with a high-resolution digital elevation model (1 m) and a 10 × 10 m model grid, to simulate flow dynamics, dam-breach timing, peak velocity, and flow depth at the depositional fan, as well as the event's temporal sequence, to support evacuation planning and the establishment of early-warning thresholds. (2) RAMMS-DF: Use the same source volumes with the high-resolution DEM (1 m) to produce deposition maps, dynamic pressure fields, and infrastructure impact assessments to support land-use planning, structural design, and emergency response preparation.

6. Discussion

6.1. Hydro-mechanical context and cascade dynamics

The Tra Leng disaster exemplifies a typical landslide hazard process in deeply weathered tropical highland catchments, where intense rainfall, fractured bedrock, thick weathering profiles, and steep terrain interact to trigger slope failure and subsequent debris-flow propagation. In the weeks before the event, persistent rainfall progressively increased soil moisture in the weathered mantle and weakened slope materials. Subsequent high-intensity rainfall is likely to have raised pore-water pressure to a critical level, triggering several slope failures in a short time. Once mobilized, the failed materials formed a debris flow that continued to incorporate colluvial deposits and channel-bed sediments as it moved through the steep, confined gorge. Upon reaching the gently sloping residential floodplain, the flow experienced a marked reduction in transport capacity, leading to rapid deceleration and extensive sediment accumulation. Geotechnical data from the boreholes confirm that both primary landslide source zones had slope angles (35-40°) that marginally exceeded the effective friction angle ($\varphi' \approx 30°$) under saturated conditions, indicating near-critical pre-failure states, and that relatively modest increases in pore pressure were sufficient to trigger failure.

6.2. Parameter transferability and model comparison with the literature

Table 2 presents the iRIC-Morpho2DH and RAMMS simulation results. The iRIC-Morpho2DH results (Vmax = 13.28 m/s, Hmax = 8.70 m) are consistent with previous research, including Asaminami's findings for the 2013 Asaminami event in Hiroshima, which reported a mean transit velocity of approximately 9 m/s (Takahashi, 2009), and documented peak velocities exceeding 8.85 m/s in a 100-year scenario at Suyukou Gully, China (Wang et al., 2025). The RAMMS-DF optimal parameters (μ = 0.205, ξ = 50 m/s^2) differ from those calibrated for alpine settings (e.g., μ = 0.07-0.11, ξ = 200-550 m/s^2) (Daud et al., 2024; Schraml et al., 2015), reflecting the lower mobility typical of short-runout tropical debris flows, which have coarser-grained material and higher void ratios.

6.3. Implications for risk management

Table 2. Comparison of key simulation outputs: iRIC-Morpho2DH vs. RAMMS-DF vs. field observations.

Parameter	iRIC-Morpho2DH	RAMMS-DF	Field Observation
Peak flow velocity (m/s)	13.28	15.12	> 10 (estimated)
Maximum flow depth (m)	8.70 (fan)	8.10 (fan)	> 8.0 (fan survey)
	21.76 (max)	22.72 (max)	> 21.0 (max)
Max. dynamic pressure (kPa)	N/A (implicit)	438.9	N/A
Natural dam height (m)	5.63 (explicit)	Not resolved	Yes, confirmed at the site
Time to fan (s)	≈ 157	N/A (no timing)	≈ 150-180*
Total event duration (s)	≈ 500	N/A	≈ 500*
Structures correctly inundated	14 / 14	14 / 14	14 (confirmed)
Deposit area (ha)	≈ 14.5 (inferred)	14.51 (explicit)	≈ 14.51 (mapped)
Validation metric	Qualitative (depth/extent)	Qualitative (depth/extent)	-
DEM resolution used	1 m	1 m	-
Explicit bed erosion	Yes (E/c* term)	No	-
Dam-breach dynamics	Yes (explicit)	No	-

Field investigations and borehole data indicate that combined antecedent (3÷4 weeks, > 1,000÷1,200 mm) and event-day (> 150÷200 mm) rainfall thresholds are sufficient to saturate the IA1 failure horizon and trigger source-zone failure. These thresholds should be formalized as the operational basis for a two-stage early-warning protocol: a preparedness alert at sustained antecedent accumulation, escalating to a mandatory evacuation warning when event-day intensity approaches critical levels, computed in near-real time from automatic rain-gauge data. RAMMS-DF pressure maps identify the Noc Ong De residential cluster as the highest-risk sub-zone (flow height 8÷10 m, pressure 200÷440 kPa), informing priority land-use restrictions and the siting of structural countermeasures, including slit check-dams in the upper channel, structures at the natural constriction point, and lateral deflection berms to redirect deposition away from residential areas.

7. Conclusions

The 28 October 2020 Tra Leng debris-flow event was investigated using a multi-source framework that integrates UAV-based terrain reconstruction, borehole-derived geotechnical characterization, and comparative numerical runout simulations using iRIC-Morpho 2 DH and RAMMS-DF. The key outcomes of the study are as follows:

(1) iRIC-Morpho 2 DH effectively captured the event's sequential development, including four primary phases of cascading slope failure and flow propagation. A key advantage of this model is its ability to explicitly simulate the formation of a temporary natural dam and its subsequent breach at approximately t = 253 s. This breaching episode generated a surge that reached a peak velocity of 13.28 m/s and a maximum flow depth of 8.70 m in the fan area. Because this model incorporates physics-based non-Newtonian flow models, bottom erosion, and temporal evolution, it is better suited for analyzing hazard intensity and temporal evolution.

(2) With the calibrated friction parameters $\mu = 0.205$ and $\xi = 50$ m/s ^{2}, RAMMS-DF predicted a maximum velocity of 15.12 m/s, a fan-area maximum flow depth of 8.10 m, an upper-gorge maximum flow depth of 22.72 m, a maximum dynamic pressure of 438.9 kPa, and a depositional area of 14.51 ha. These results are consistent with field-mapped evidence.

(3) A comparison between the two models suggests that both codes should be considered. iRIC-Morpho is more effective at capturing transient flow mechanisms and process accuracy, while RAMMS-DF is more practical for rapid deposition mapping.

(4) This study has the disadvantage of lacking accurate UAV and DEM data before the debris flow occurs. In addition, the RAMMS software includes several parameters that have not been

directly identified from the experimental results. In the future, it is necessary to establish warning thresholds or build structures to minimize the impact of debris flows in mountainous areas.

Acknowledgements

This research was funded by the Vietnamese National Foundation for Science and Technology Development (NAFOSTED), Grant No. 105.08-2021.74 (Principal Investigator: Assoc. Prof. Dr. Nguyen Chau Lan).

Contributions of authors

Chau Lan Nguyen - methodology, writing, review & supervision; Van Kien Vu - writing, modelling; Tuan Nghia Do - writing, review & editing, supervision.

References

Abraham, M., Satyam, N., Pradhan, B., & Tian, H. (2022). Debris flow simulation 2D (DFS 2D): Numerical modelling of debris flows and calibration of friction parameters. *Journal of Rock Mechanics and Geotechnical Engineering, 14*. doi:https://doi.org/10.1016/j.jrmge.2022.01.004.

Ahmad, N., Shafique, M., Hussain, M. L., & Ullah, I. (2025). Integrated debris flow hazard and risk assessment using UAV data and RAMMS, a case study in northern Pakistan. *Natural Hazards, 121*(2), 1463-1487. doi:https://doi.org/10.1007/s11069-024-06862-0.

Bui, Q. D., Do, D., Pham, Q. D., Ha, H., Nguyen, L. P., Duong, H. C., . . . Luu, C. (2026). UAV-based topography and RAMMS-DF simulation for debris flow impact assessment: Insights from the typhoon Molave in Phuoc Thanh commune of Vietnam. *Geomatica, 78*(1), 100091. doi:https://doi.org/10.1016/j.geomat.2026.100091.

Chen, C. Y., & Wang, Q. (2017). Debris flow-induced topographic changes: effects of recurrent debris flow initiation. *Environ Monit Assess, 189*(9), 449. doi:https://doi.org/10.1007/s10661-017-6169-y.

Chen, H., Xiong, J., Zhao, W., Chen, J., Zhang, X., Ruan, H., . . . Gong, L. (2024). Catastrophic debris flow triggered by a June 26, 2023 rainstorm suggests the debris flow is still active 15 years after the Wenchuan seismic. *Landslides, 21*(8), 1883-1897. doi:https://doi.org/10.1007/s10346-024-02279-9.

Daud, H., Tanoli, J. I., Asif, S. M., Qasim, M., Ali, M., Khan, J., . . . Jadoon, I. A. K. (2024). Modelling of debris-flow susceptibility and propagation: a case study from Northwest Himalaya. *Journal of Mountain Science, 21*(1), 200-217. doi:https://doi.org/10.1007/s11629-023-7966-0.

He, S., Wang, D., Li, Y., Zhao, P., Lan, H., Chen, W., . . . Chen, X. (2021). Social-ecological system resilience of debris flow alluvial fans in the Awang basin, China. *Journal of Environmental Management, 286*, 112230. doi:https://doi.org/10.1016/j.jenvman.2021.112230.

Imaizumi, F., Hayakawa, Y., Hotta, N., Tsunetaka, H., Ohsaka, O., & Tsuchiya, S. (2017). Relationship between the accumulation of sediment storage and debris-flow characteristics in a debris-flow initiation zone, Ohya landslide body, Japan. *Natural Hazards and Earth System Sciences, 17*, 1923-1938. doi:https://doi.org/10.5194/nhess-17-1923-2017.

Iverson, N. R., Cohen, D., Hooyer, T. S., Fischer, U. H., Jackson, M., Moore, P. L., . . . Kohler, J. (2003). Effects of basal debris on glacier flow. *Science, 301*(5629), 81-84. doi:https://doi.org/10.1126/science.1083086.

Iverson, R. M. (1997). The physics of debris flows. *Reviews of geophysics, 35*(3), 245-296. doi:https://doi.org/10.1029/97RG00426.

Jakob, M., Hungr, O., & Jakob, D. M. (2005). *Debris-flow hazards and related phenomena* (Vol. 739): Springer.

Jakob, M., Stein, D., & Ulmi, M. (2012). Vulnerability of buildings to debris flow impact. *Natural Hazards, 60*(2), 241-261.

doi:https://doi.org/10.1007/s11069-011-0007-2.

Lan, N. C., Nghĩa, Đ. T., Tiền, P. V., Kiên, N. T., Kiên, V. V., Thành, B. T., & Long, N. N. (2024). *Debris-flow study in Tra Leng, Quang Nam Province using Kanako 1D software and proposal of suitable engineering solutions, National Conference on Earth Sciences and Resources for Sustainable Development.* Paper presented at the ERSD 2024, Engineering Geology and Geotechnical Engineering.

Mikoš, M., & Bezak, N. (2021). Debris Flow Modelling Using RAMMS Model in the Alpine Environment With Focus on the Model Parameters and Main Characteristics. *Volume 8 - 2020*. doi:https://doi.org/10.3389/feart.2020.605061.

Schraml, K., Thomschitz, B., McArdell, B., Graf, C., & Kaitna, R. (2015). Modeling debris-flow runout patterns on two alpine fans with different dynamic simulation models. *Natural Hazards and Earth System Sciences, 15*. doi:https://doi.org/10.5194/nhess-15-1483-2015.

Singh, M., Chattoraj, S. L., & Das, R. (2025). Integrated Landslide Hazard Assessment Using Machine Learning, Rainfall Threshold, and RAMMS Based Rockfall Simulation in NH-05, Himachal Pradesh, India. *Journal of the Indian Society of Remote Sensing, 53*(11), 3813-3842. doi:https://doi.org/10.1007/s12524-025-02173-4.

Takahashi, T. (1978). Mechanical characteristics of debris flow. *Journal of the Hydraulics Division, 104*(8), 1153-1169.

Takahashi, T. (2009). A review of Japanese debris flow research. *International Journal of Erosion Control Engineering, 2*(1), 1-14. doi:https://doi.org/10.13101/ijece.2.1.

Takebayashi, H., & Fujita, M. (2020). Numerical Simulation of a Debris Flow on the Basis of a Two-Dimensional Continuum Body Model. *geosciences, 10*(2), 45. doi:https://doi.org/10.3390/geosciences10020045.

Wang, G., Wang, H., He, Z., Gao, S., Zhang, G., Hu, Z., . . . Yan, J. (2025). Numerical Simulation and Risk Assessment of Debris Flows in Suyukou Gully, Eastern Helan Mountains, China. *17*(13), 5984. doi:https://doi.org/10.3390/su17135984.